Exploring Phase Coherence in a 2D Lattice of Bose-Einstein Condensates

Markus Greiner, Immanuel Bloch, Olaf Mandel, Theodor W. Hänsch,* and Tilman Esslinger
Sektion Physik, Ludwig-Maximilians-Universität, Schellingstrasse 4/III, D-80799 Munich, Germany and Max-Planck-Institut für Quantenoptik, D-85748 Garching, Germany
(Received 4 May 2001; published 1 October 2001)

Bose-Einstein condensates of rubidium atoms are stored in a two-dimensional periodic dipole force potential, formed by a pair of standing wave laser fields. The resulting potential consists of a lattice of tightly confining tubes, each filled with a 1D quantum gas. Tunnel coupling between neighboring tubes is controlled by the intensity of the laser fields. By observing the interference pattern of atoms released from more than 3000 individual lattice tubes, the phase coherence of the coupled quantum gases is studied. The lifetime of the condensate in the lattice and the dependence of the interference pattern on the lattice configuration are investigated.

DOI: 10.1103/PhysRevLett.87.160405 PACS numbers: 03.75.Fi, 03.65.Nk, 05.30.Jp, 32.80.Pj

The physics of Bose-Einstein condensation is governed by a hierarchy of energy scales. The lowest energy is usually the atomic oscillation frequency in the trap which is much smaller than the chemical potential of the condensate. Here we report on experiments in which we enter a regime where this order is inverted. By overlapping two optical standing waves with the magnetically trapped condensate we create a two-dimensional periodic lattice of tightly confining potential tubes. In each of the several thousand tubes the chemical potential is far below the trapping frequencies in the radial direction. The radial motion of the atoms is therefore confined to zero point oscillations, and transverse excitations are completely frozen out. In the degenerate limit, these 1D quantum gases are expected to show a remarkable physics not encountered in 2D and 3D, for instance, a continuous crossover from bosonic to fermionic behavior as the density is lowered [1–5].

In our two-dimensional periodic array of quantum gases the tunnel coupling between neighboring lattice sites is controlled with a high degree of precision by changing the intensity of the optical lattice beams. A similar control over coupling between adjacent pancake-shaped condensates was achieved in recent experiment using a single standing wave laser field [6,7]. After suddenly releasing the atoms from the trapping potential we observe the multiple matter wave interference pattern of several thousand expanding quantum gases. This allows us to study the phase coherence between neighboring lattice sites, which is remarkably long lived. Even for long storage times, when the phase coherence between neighboring lattice sites is lost and no interference pattern can be observed anymore, the radial motion of the atoms remains confined to zero point oscillations.

Similar to our previous work [8], almost pure Bose-Einstein condensates with up to 5×10^5 ^{87}Rb atoms are created in the $|F = 2, m_F = 2\rangle$ state. The cigar-shaped condensates are confined in the harmonic trapping potential of a QUIC trap (a type of magnetic trap that incorporates the quadrupole and Ioffe configuration) [9] with an axial trapping frequency of 24 Hz and radial trapping frequencies of 220 Hz. The lattice potential is formed by overlapping two perpendicular optical standing waves with the Bose-Einstein condensate as shown in Fig. 1. All lattice beams are derived from the output of a laser diode operating at a wavelength of $\lambda = 852$ nm and have spot sizes w_0 ($1/e^2$ radius for the intensity) of approximately 75 μm at the position of the condensate. The resulting potential for the atoms is directly proportional to the intensity of the interfering laser beams [10], and for the case of linearly polarized light fields it can be expressed by

$$U(y,z) = U_0\{\cos^2(ky) + \cos^2(kz) + 2\mathbf{e}_1 \cdot \mathbf{e}_2 \cos\phi \cos(ky)\cos(kz)\}. \quad (1)$$

Here U_0 describes the potential maximum of a single standing wave, $k = 2\pi/\lambda$ is the magnitude of the wave vector of the lattice beams, and $\mathbf{e}_{1,2}$ are the polarization vectors of the horizontal and vertical standing wave laser fields, respectively. The potential depth U_0 is conveniently measured in units of the recoil energy $E_r = \hbar^2 k^2/2m$, with m being the mass of a single atom. The time-phase difference between the two standing waves is given by the

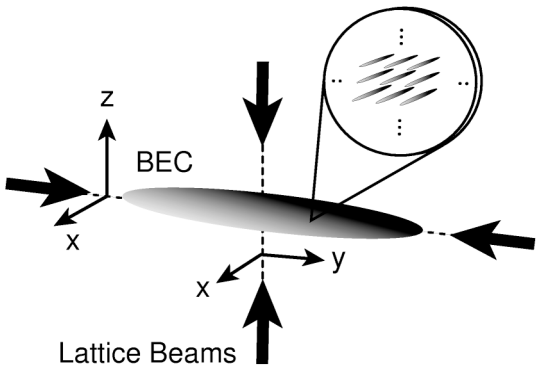

FIG. 1. Schematic setup of the experiment. A 2D lattice potential is formed by overlapping two optical standing waves along the horizontal axis (y axis) and the vertical axis (z axis) with a Bose-Einstein condensate in a magnetic trap. The condensate is then confined to an array of several thousand narrow potential tubes (see inset).

variable ϕ [11]. In our setup this time phase is measured interferometrically and controlled with a piezomounted mirror and a servoloop. Furthermore, the intensity of the lattice beams is stabilized in order to ensure a constant potential depth during our measurements. The intensity pattern in the y-z plane extends along the x direction, such that the resulting potential can be viewed as a lattice of narrow tubes with a spacing of $\lambda/2$ between neighboring lattice sites. These tubes provide a tight harmonic confinement along the radial direction which leads to large trapping frequencies $\omega_r \approx \hbar k\sqrt{2U_0/m}$. In our setup potential depths of up to $12E_r$ are reached, resulting in a maximum radial trapping frequency of $\omega_r \approx 2\pi \times 18.5$ kHz. The confinement along the symmetry axis of a single tube is determined by the harmonic confinement of the magnetic trap and the confinement due to the Gaussian intensity profile of the lattice laser beams. The trapping frequency along the symmetry axis of a single lattice tube can be varied between $\omega_{\mathrm{ax}} \approx 2\pi \times 10$–$300$ Hz. The spontaneous scattering rate due to the lattice laser light is always less than $\Gamma_{\mathrm{sc}} = 0.06\ \mathrm{s}^{-1}$ and therefore negligible for our measurement times.

In order to transfer the atoms into the lattice potential, the laser power of the lattice beams is gradually increased in a linear ramp to its final strength within 40 ms. The atoms are then held for a variable amount of time in the combined potential of the interfering laser beams and the magnetic trap. The number of occupied lattice sites can be estimated by counting the number of lattice sites within the Thomas-Fermi extension of the magnetically trapped condensate. For the above parameters we find that up to 3000 lattice sites are populated, with an average population of $\bar{N}_i \approx 170$ atoms per lattice site.

When the atoms are released from the combined potential of the optical lattice and the magnetic trap, the condensate wave functions on different lattice sites expand and interfere with each other. This interference pattern is imaged after a fixed expansion time using absorption imaging, with the imaging axis oriented along the x axis and positioned parallel to the symmetry axis of the individual lattice tubes. The results are displayed in Fig. 2 for a 2D-lattice potential with a maximum potential depth of $12E_r$ and orthogonal polarization vectors $\mathbf{e}_1 \cdot \mathbf{e}_2 = 0$. In comparison, Fig. 3 shows the results for three different potential depths of the optical lattice and 1D vertical (z axis), 1D horizontal (y axis), and 2D vertical+horizontal lattice configurations (orthogonal polarization vectors $\mathbf{e}_1 \cdot \mathbf{e}_2 = 0$). Several important features can be seen on these images. First, discrete interference maxima are visible that are arranged in a regular structure. These interference maxima not only require a periodic density modulation of the atoms but also phase coherence of the condensate wave function throughout the lattice. They directly reveal the momentum distribution of the atoms in the lattice. Second, s-wave scattering spheres [12,13] become more visible as the higher order momentum components are more strongly populated with increasing potential depth. These scattering spheres occur due to collisions between atoms in the separating momentum components after the trapping potential is switched off. The collision probability between atoms in the horizontal momentum components $|p_y| = 2\hbar k$ and the $|p| = 0$ momentum component is high, due to the large extension of the condensate in the horizontal direction. This yields long interaction times and thus a high scattering probability. Along the vertical direction, the size of the condensate is almost an order of magnitude smaller and the interaction times are correspondingly shorter, resulting in a much lower scattering probability. Furthermore, s-wave scattering spheres can also be seen in the diagonal direction due to collisions between the diagonal momentum components and the central $p = 0\hbar k$ momentum component. For a maximum trapping depth of $12E_r$ all of these eight scattering spheres [see Fig. 2(b)] are clearly visible in Fig. 2(a). For the parameters used in our experiment the photon scattering rate is 2 orders of magnitude

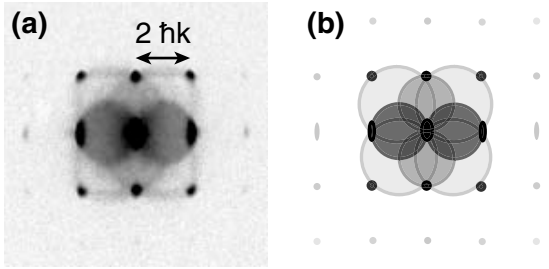

FIG. 2. (a) Average over 5 absorption images of released Bose-Einstein condensates that were stored in a 2D optical lattice potential. The maximum potential depth of the lattice was $12E_r$ and the ballistic expansion time was set to 12 ms. (b) Schematic image showing the expected discrete momentum states and the possible s-wave scattering spheres. Higher order momentum components (e.g., $4\hbar k$) are also visible in (a).

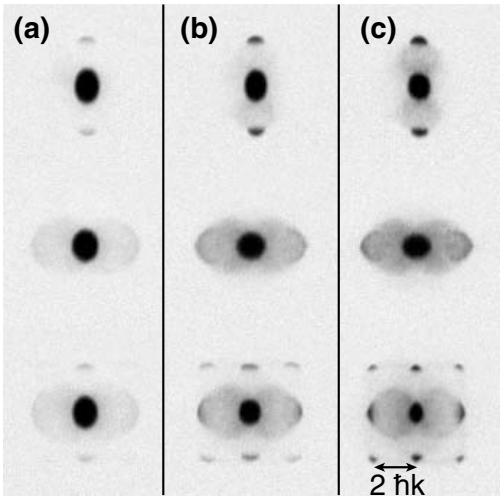

FIG. 3. Absorption images of Bose-Einstein condensates released from optical lattices of different geometry and intensity. Top row: One-dimensional lattice oriented vertically. Middle row: One-dimensional lattice oriented horizontally. Bottom row: Two-dimensional lattice oriented along the vertical and horizontal direction. The images were taken for peak optical lattice depths of (a) $4E_r$, (b) $8E_r$, and (c) $12\ E_r$.

below that in Ref. [14], so that superradiant effects should not occur. Because of the symmetry of our standing wave field we do not expect additional momentum components to be generated by four-wave mixing [15].

The wave function of the Bose-Einstein condensate in the optical lattice can be expressed as a sum of localized wave functions on each lattice site. Such a localized wave function is described by a Gaussian wave function for the ground state of the tightly confining radial axis of a single lattice tube, with radial widths as low as 90 nm. Along the weakly confining axis of a lattice tube, the repulsive interactions between the atoms result in a parabolic Thomas-Fermi profile with a maximum radial width of $\approx 5\mu$m. The maximum chemical potential per lattice tube of $\mu \approx h \times 6$ kHz is then much smaller than the radial energy level spacing, confining the radial atomic motion to zero point oscillations.

In addition to a strong dependence of the visibility of the higher order momentum components on the localization of the wave function, we find a suppression of momentum components due to structural properties of the optical lattice. For a lattice configuration with orthogonal polarization vectors between the two standing waves for which the last term in the sum of Eq. (1) vanishes [see Fig. 4(a)], the first order diagonal momentum components with $|p| = \sqrt{2}\,\hbar k$ are completely suppressed, as can be seen in Fig. 4(b). This is caused by a destructive interference between matter waves emitted from neighboring diagonal lattice planes and results in a vanishing geometrical structure factor of these momentum components [16]. If the lattice configuration is changed to parallel polarization vectors between the two standing waves, such that $\mathbf{e}_1 \cdot \mathbf{e}_2 = 1$, and the time phase is set to $\phi = 0$, the last term in Eq. (1) modifies the geometry of the lattice [see Fig. 4(c)]. For this lattice configuration the geometrical structure factor for the diagonal momentum components with $|p| = \sqrt{2}\,\hbar k$ does not vanish, and these components are clearly visible in the experiment [see Fig. 4(d)].

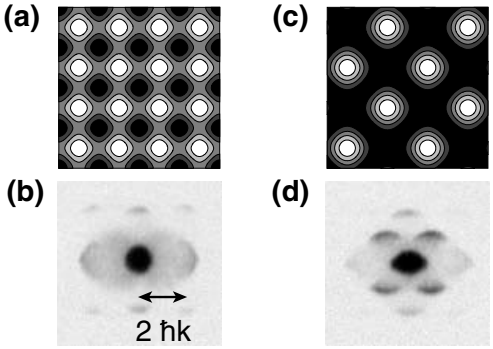

FIG. 4. Influence of the lattice configuration on the momentum distribution. For an optical lattice of (a) with orthogonal polarization vectors $\mathbf{e}_1 \cdot \mathbf{e}_2 = 0$ the first diagonal momentum orders with $|p| = \sqrt{2}\,\hbar k$ are suppressed (b) due to their vanishing geometrical structure factor. In contrast, if $\mathbf{e}_1 \cdot \mathbf{e}_2 = 1$ and $\phi = 0$ as in (c), the resulting geometrical structure factor does not vanish for these momentum components and they are strongly visible (d).

We determine the lifetime of the condensate in the optical lattice by measuring the number of condensed atoms after ramping down the lattice potential. The following experimental sequence is used. The lattice is ramped up to its final strength within 40 ms and then the atoms are held for a variable period of time in the lattice potential. Subsequently, the lattice potential is ramped down within 40 ms and the remaining number of condensed atoms is measured using absorption imaging after a ballistic expansion. The slow ramp speed ensures that the many-body wave function adjusts adiabatically to the changing optical potential. The results of these measurements are displayed in Fig. 5 for a lattice configuration with orthogonal polarization vectors $\mathbf{e}_1 \cdot \mathbf{e}_2 = 0$ [see Fig. 4(a)]. The reduction of the lifetime of the condensate due to the presence of the optical lattice is shown for three different potential depths. We believe that this reduced lifetime is caused by residual fluctuations of the lattice potential which lead to a dephasing of neighboring condensates with time. In a deep potential the dephasing occurs faster due to the reduced tunnel coupling. This may also be considered in a band structure picture, where the width of the energy bands decreases strongly with increasing potential depth, so that the system becomes more susceptible to perturbations. As a result, transitions within a single band may occur; i.e., the atoms remain within the ground state of a single lattice site, but no longer exhibit phase coherence to neighboring sites. The dephased Bose-Einstein condensates are not expected to recombine into a single condensate when the optical lattice potential is turned off adiabatically. We identify this as the major contribution to the observed decrease in condensate fraction with increasing storage time. We have also verified that the remaining condensate fraction and the interference pattern after a sudden switch-off vanish for the same parameters and holding times. Because of the background of atoms which undergo s-wave

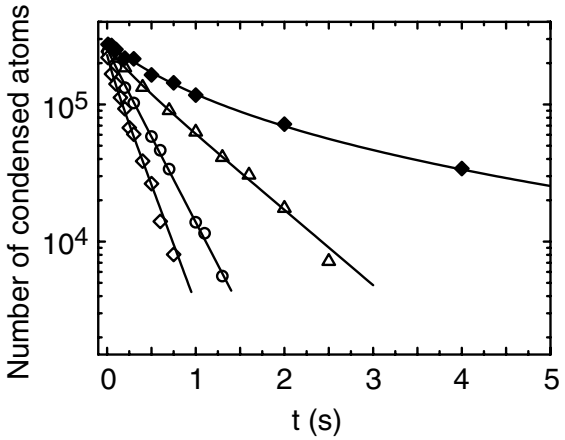

FIG. 5. Remaining number of condensed atoms after a variable hold time in the combined potential of the magnetic trap and the lattice potential (open data points) and in a pure magnetic trapping potential (solid diamonds). The maximum potential depth of the lattice was $4E_r$ (open triangles), $8E_r$ (open circles), and $12E_r$ (open diamonds), respectively.

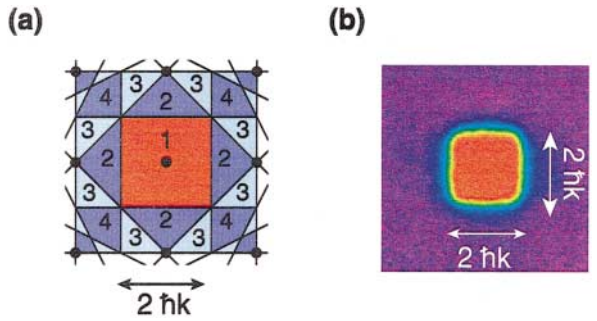

FIG. 6 (color). (a) Reciprocal lattice and Brillouin zones for the two-dimensional Bravais lattice of Fig. 4(a). (b) False color image of the experimentally measured band population of a dephased Bose-Einstein condensate in a $12E_r$ deep optical lattice where phase coherence between neighboring lattice sites has been lost.

scattering, the measurement of the interference pattern is less suitable to quantitatively analyze the coherent fraction of atoms in the lattice.

The dephasing of the condensate wave function in the optical lattice becomes clearly visible when we introduce an external perturbation by switching off the magnetic trapping field and thereby exposing the atoms to the linear gravitational potential. For a $12E_r$ deep optical lattice and 2 ms after switching off the magnetic field we can no longer observe an interference pattern in the density distribution of the released atoms. This indicates that phase coherence of the atoms across the lattice has been lost. To experimentally determine which energy bands are populated by the dephased Bose-Einstein condensate, we ramp down the optical potential in 2 ms, after the 2 ms hold time in the pure optical potential. This ramp speed ensures that we are adiabatic with respect to the atomic motion in a single lattice site and preserve the band population. The momentum distribution of the atomic cloud is obtained by imaging the atoms after 12 ms of ballistic expansion. Atoms originating from the lowest energy band are then expected to obtain momenta that lie within the first Brillouin zone of the lattice [17]. The Brillouin zones of a two-dimensional Bravais lattice are displayed in Fig. 6(a). The experimentally measured momentum distribution shown in Fig. 6(b) exhibits a pronounced squarelike momentum distribution of width $2\hbar k$ coinciding with the first Brillouin zone of the Bravais lattices. This proves that the atoms from the dephased condensate populate only the lowest energy band of the lattice and remain in the radial ground state of a single lattice tube even if the phase coherence between neighboring lattice sites has vanished.

Employing the same method we have measured the band population in the combined potential of the magnetic trap and the optical lattice. For a $12E_r$ deep lattice and after a storage time of 1 s we find that 60% of the initial number of atoms are still present and that all of these atoms remain confined to the first energy band. For the same parameters no significant condensate fraction was measured (see Fig. 5). So far, we cannot identify whether axial excitations are present in a single lattice tube.

In conclusion, we have created an experimental system which now enables us to study the physics of ultracold 1D quantum gases (see also [18]). A variety of fundamental questions of the physics in reduced dimensions can now be addressed in the experiment. The correlation properties of 1D quantum gases are intrinsically different from those encountered in 3D. It is expected that in a 1D gas the decrease of temperature leads to a continuous transformation of the correlation properties from the ideal gas case to the regime which is dominated by quantum statistics and interactions [4]. In the extreme limit of low atomic densities or large interactions even the character of the bosonic particles changes and the gas acquires Fermi properties [1–5].

By adding a further standing wave laser field we can extend the geometry of the lattice to three dimensions. This should pave the way towards the observation of a quantum phase transition in a dilute gas of atoms from a superfluid to a Mott insulator phase [19]. We believe that straightforward modification of our experiment should allow us to reach this regime.

We thank Wilhelm Zwerger and Martin Holthaus for stimulating discussions and Anton Scheich for experimental assistance during the construction of the experiment. We also acknowledge support by the Deutsche Forschungsgemeinschaft.

*Also at Department of Physics, University of Florence, Italy.

[1] M. Girardeau, J. Math. Phys. (N.Y.) **1**, 516 (1960).
[2] E. H. Lieb and W. Liniger, Phys. Rev. **130**, 1605 (1962); E. H. Lieb, Phys. Rev. **130**, 1616 (1963).
[3] M. Olshanii, Phys. Rev. Lett. **81**, 938 (1998).
[4] D. S. Petrov, G. V. Shlyapnikov, and J. T. M. Walraven, Phys. Rev. Lett. **85**, 3745 (2000).
[5] M. D. Girardeau, E. M. Wright, and J. M. Triscari, Phys. Rev. A **63**, 033601 (2001).
[6] B. P. Anderson and M. A. Kasevich, Science **281**, 1686 (1998).
[7] C. Orzel *et al.,* Science **291**, 2386 (2001).
[8] M. Greiner, I. Bloch, T. W. Hänsch, and T. Esslinger, Phys. Rev. A **63**, 031401 (2001).
[9] T. Esslinger, I. Bloch, and T. W. Hänsch, Phys. Rev. A **58**, 2664 (1998).
[10] R. Grimm, M. Weidemüller, and Y. B. Ovchinnikov, Adv. At. Mol. Opt. Phys. **42**, 95–170 (2000), and references therein.
[11] A. Hemmerich *et al.,* Europhys. Lett. **18**, 391 (1992).
[12] Y. B. Band *et al.,* Phys. Rev. Lett. **84**, 5462 (2000).
[13] A. P. Chikkatur *et al.,* Phys. Rev. Lett. **85**, 483 (2000).
[14] S. Inouye *et al.,* Science **285**, 571 (1999).
[15] L. Deng *et al.,* Nature (London) **398**, 218 (1999).
[16] See, for example, N. W. Ashcroft and N. D. Mermin, *Solid State Physics* (Saunders College Publishing, Fort Worth, TX, 1976).
[17] A. Kastberg *et al.,* Phys. Rev. Lett. **74**, 1542 (1995).
[18] A. Görlitz *et al.,* cond-mat/0104549.
[19] D. Jacksch *et al.,* Phys. Rev. Lett. **81**, 3108 (1998).